Structural, electronic, and magnetic properties of $LaNi_{5-x}T_x$ (T=Fe,Mn) compounds

J. B. Yang
Materials Research Center, University of Missouri–Rolla, Rolla, Missouri 65409

C. Y. Tai, G. K. Marasinghe, and G. D. Waddill
Materials Research Center and Department of Physics, University of Missouri–Rolla, Rolla, Missouri 65409

O. A. Pringle
Department of Physics, University of Missouri–Rolla, Rolla, Missouri 65409

W. J. James
Materials Research Center and Department of Chemistry, University of Missouri–Rolla, Rolla, Missouri 65409

Y. Kong
Max-Planck-Institut für Festkörperforschung, Heisenbergstrasse 1, D-70569, Stuttgart, Germany
(Received 18 July 2000; published 11 December 2000)

Structures and magnetic properties of the $LaNi_{5-x}Fe_x$ and $LaNi_{5-x}Mn_x$ compounds have been investigated using neutron diffraction and first-principles tight-binding-linear-muffin-tin-orbital methods. Both neutron diffraction refinement data and total energy calculations show that the Fe and Mn atoms preferentially occupy the $3g$ sites in the hexagonal $CaCu_5$-type structure. The calculated magnetic moments of Fe and Ni atoms are of $2.4–2.5\mu_B$ and $0.2–0.5\mu_B$ in $LaNi_{5-x}Fe_x$, respectively. The magnetic structure exhibits more localized moments at Fe atoms in $LaNi_{5-x}Fe_x$ when $x \leqslant 1.0$. Electronic structure calculations indicate that *s*-conduction electron spin polarization from the Ni or La atoms strongly interacts with Fe(Mn) *d*-spin moments in $LaNi_{5-x}Fe(Mn)_x$ ($x \neq 0$) compounds, which gives rise to a very large valence transferred hyperfine field on the Ni or La sites. This *s*-*d* hybridization may lead to an interaction among magnetic clusters in these kinds of materials and may cause a spin freezing effect at low temperature when the Fe(Mn) content is very low in $LaNi_{5-x}Fe(Mn)_x$. Mn atoms show magnetic moments of $3.0\mu_B$ per atom due to a large exchange splitting in $LaNi_{5-x}Mn_x$ ($x \neq 0$). $LaNi_4Mn$ is found to be ferrimagnetic, whereas antiferromagnetic exchange coupling between the Mn atoms is preferred for $LaNi_3Mn_2$. Both ferrimagnetic and ferromagnetic exchange interactions between Mn atoms are found in the $LaNi_2Mn_3$ compounds. The calculated results are in good agreement with the experimental neutron data.

DOI: 10.1103/PhysRevB.63.014407 PACS number(s): 75.50.Gg, 31.15.Ar, 75.20.Hr, 61.12.Ld

I. INTRODUCTION

The investigation of the R-T (R=rare earth, T=transition metal) interaction in $4f$-$3d$ intermetallic compounds has been the subject of many theoretical and experimental studies.[1–3] The R-T compounds are known to show interesting magnetic properties associated with both localized moments of rare earth atoms and itinerant electrons of the $3d$ atoms.[4] There is considerable interest in the electronic structure of $LaNi_5$ in regard to both its high capacity for hydrogen absorption[5] and in its feature of having exchange-enhanced susceptibility.[6] $LaNi_5$ possesses the hexagonal $CaCu_5$ structure(space group $P6/mmm$) with one formula unit (f.u.) per unit cell. This crystal structure is extremely simple (see Fig. 1), with Ni atoms occupying two different crystallographic sites, $3g$ and $2c$, and La occupying the $1a$ sites. The $LaFe_5$ and $LaMn_5$ intermetallics do not exist, however, series of solid solutions exist for $La(Ni,Fe)_5$ and $La(Ni,Mn)_5$,[7–18] which provide for the study of the magnetic properties of $3d$ electrons in these compounds. Both of these series show some special magnetic features which depend upon the concentration of Mn and Fe, such as spin glass behavior, which has been observed at low temperature when some amount of Ni is substituted by Fe or Mn.[12–14]

In order to study the structural and magnetic properties of $LaNi_{5-x}T_x$ (T=Fe,Mn) and investigate the effect of the local environment on the magnetic properties, neutron diffraction measurements of $LaNi_{5-x}Fe_x$ ($0 \leqslant x \leqslant 1.4$) and $LaNi_{5-x}Mn_x$ ($0 \leqslant x \leqslant 2.0$) have been carried out to determine

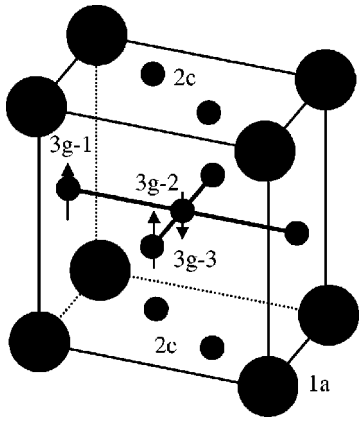

FIG. 1. The $CaCu_5$ type structure of $LaNi_{5-x}T_x$ (T=Fe,Mn). The large atoms are La, and the smaller atoms are Ni, Fe, or Mn.

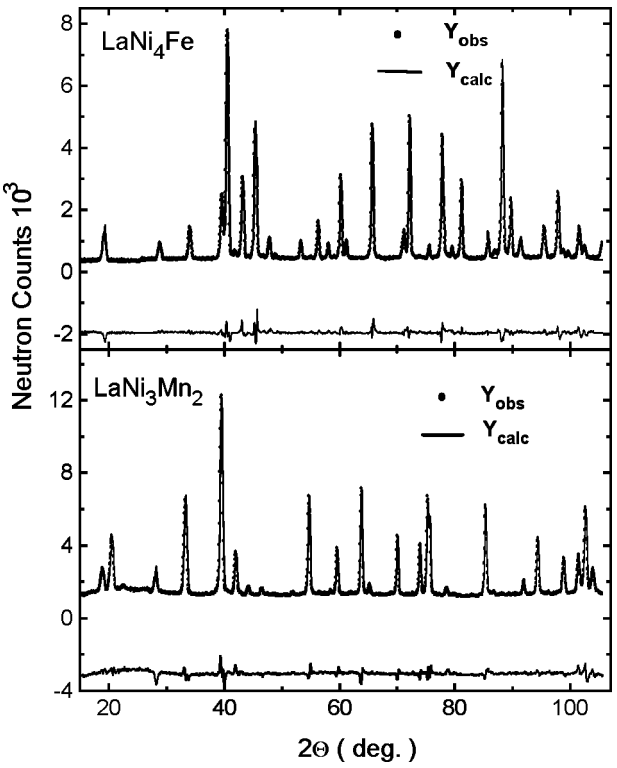

FIG. 2. The typical neutron diffraction patterns of $LaNi_4Fe$ at 20 K and $LaNi_3Mn_2$ at 30 K. The bottom curves are the difference between experimental data and refinement data.

the crystallographic structures,[17] and first-principles tight-binding linear-muffin-tin-orbital (TB-LMTO) method has been applied to calculate electronic structure of $LaNi_{5-x}Fe_x$ and $LaNi_{5-x}Mn_x$. Based on the results of the spin-polarization calculations, the site preference and magnetic moments, as well as the hyperfine fields at nuclei have been obtained and compared with experimental results.

After presenting the neutron diffraction patterns and refinement data of the crystallographic structures and magnetic moments in Sec. II, some computational details are described in Sec. III. The calculated electronic structures, magnetic properties, and the hyperfine fields are presented in Sec. IV together with further discussion and comparison with experimental results.

II. CRYSTALLOGRAPHIC STRUCTURES AND MAGNETIC MOMENTS

$LaNi_{5-x}Fe_x$ and $LaNi_{5-x}Mn_x$ samples were prepared from elements with a purity of 99.99% or better by induction melting in a cold boat copper crucible followed by annealing at 950 °C for one week. Both x-ray diffraction and neutron diffraction were used to determine the structures of these compounds. Neutron diffraction data were collected at low temperature and room temperature at the University of Missouri research reactor and analyzed by a Rietveld structure refinement program[19]. Figure 2 shows the typical neutron diffraction patterns of $LaNi_4Fe$ at 20 K and $LaNi_3Mn_2$ at 30 K. All samples crystallize in the $CaCu_5$-type structure. Figure 3 is a plot of the lattice parameters a and c of the

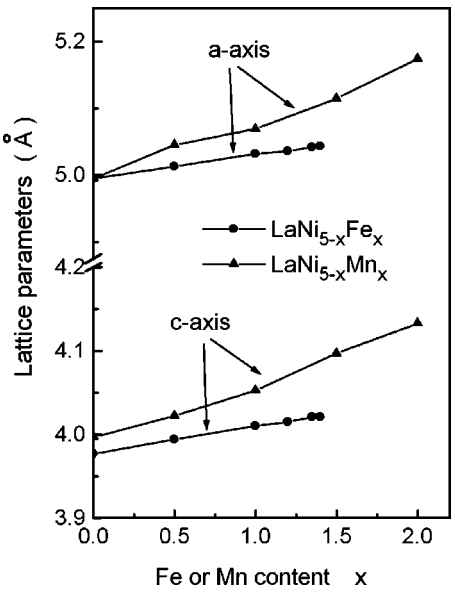

FIG. 3. The lattice parameters *a* and *c* of $LaNi_{5-x}Fe_x$ and $LaNi_{5-x}Mn_x$ compounds.

$LaNi_{5-x}Fe_x$ and $LaNi_{5-x}Mn_x$ compounds. It is found that Mn and Fe substitution results in an increase of the lattice parameters. The relative unit cell volume expansion ratios are about 2.5% per Fe atom and 5.5% per Mn atom. The larger expansion rate of Mn compounds is due to the larger atomic radius of Mn($R_{\mathrm{Mn}}=1.31$ Å) relative to Fe($R_{\mathrm{Fe}}=1.27$ Å). The magnetic moments of the atoms were refined by fixing all the crystallographic parameters. The magnetic moment of the La atom is fixed to zero for all compounds. The refined atomic coordinates and average magnetic moments on all sites are listed in Table I. From Table I, it is shown that the Fe and Mn atoms preferably occupy the $3g$ sites consistent with the finding of the most previous studies.[9,10,13] For the $LaNi_{5-x}Fe_x$ compounds, the total magnetization increases with the Fe content. Since Ni is nonmagnetic in $LaNi_5$, a small magnetic moment on Ni atoms, which increases with the Fe content, is induced by magnetic Fe atoms. The increase of Ni magnetic moment with Fe content is attributed to the enhanced Fe-Ni exchange interaction, and is confirmed by the increase of the Curie temperature in $LaNi_{5-x}Fe_x$.[17] For the $LaNi_{5-x}Mn_x$ compounds, the average magnetic moments of the Mn atoms are 3.25, 3.0, and $2.45\mu_B$ for $x=1.0$, 1.5, and 2.0, respectively. The $LaNi_4Mn$ compound has the highest magnetization of $3.94\mu_B$/f.u., while the net magnetization of $LaNi_{3.5}Mn_{1.5}$ is $1.86\mu_B$/f.u. The net magnetization of $LaNi_3Mn_2$ tends to zero. The decrease of magnetization is due to ferrimagnetic or antiferromagnetic exchange coupling between Mn atoms in the samples with *x* larger than 1.0. The magnetic moments of Ni atoms in $LaNi_{5-x}Mnx$ compounds are very small and decrease to nearly zero when $x=2.0$.

III. COMPUTATIONAL DETAILS

The self-consistent TB-LMTO atomic-sphere-approximation (ASA) method has been employed to perform

TABLE I. Refinement parameters of $LaNi_{5-x}Fe_x$ ($x=1.0$ and 1.4) at 20 K and $LaNi_{5-x}Mn_x$ ($x=1.0$ and 2.0) at 30 K. n is the occupation factor; x, y, z are the fractional position coordinates; m is the magnetic moment (μ_B). R_{Bragg} is the Bragg R factor, R_{exp} is statistically expected residual error of entire measured scatting patterns, R_{mag} is also Bragg R factor but applied to magnetic intensities.

	$R_{\mathrm{Bragg}}=4.01\%$ $R_{wp}=6.79\%$, $R_{\mathrm{exp}}=3.57\%$				
$LaNi_4Fe$	n	x	y	z	m
La($1a$)	1	0	0	0	0
Ni($2c$)	1	2/3	1/3	0	0.36
Ni($3g$)	0.67	0.5	0.5	0.5	0.36
Fe($3g$)	0.33	0.5	0.5	0.5	2.11
$LaNi_{3.6}Fe_{1.4}$	$R_{\mathrm{Bragg}}=2.91\%$ $R_{wp}=7.33\%$ $R_{\mathrm{exp}}=2.48\%$				
La($1a$)	1	0	0	0	0
Ni($2c$)	1	2/3	1/3	0	0.48
Ni($3g$)	0.53	0.5	0.5	0.5	0.48
Fe($3g$)	0.47	0.5	0.5	0.5	2.09
$LaNi_4Mn$	$R_{\mathrm{Bragg}}=4.34\%$ $R_{wp}=4.64\%$, $R_{\mathrm{exp}}=3.85\%$				
La($1a$)	1	0	0	0	0
Ni($2c$)	1	2/3	1/3	0	0.21
Ni($3g$)	0.67	0.5	0.5	0.5	0.14
Mn($3g$)	0.33	0.5	0.5	0.5	3.25[a]
$LaNi_3Mn_2$	$R_{\mathrm{Bragg}}=5.13\%$ $R_{wp}=5.69\%$, $R_{\mathrm{exp}}=2.36\%$				
La($1a$)	1	0	0	0	0
Ni($2c$)	1	2/3	1/3	0	0.04
Ni($3g$)	0.33	0.5	0.5	0.5	0.06
Mn($3g$)	0.67	0.5	0.5	0.5	2.45[a]

[a]The Mn moments given in Ref. 17 were smaller than given in this table due to the failure to take into account the absence of a center symmetry in the magnetic unit cell.

a scalar relativistic band calculation in the framework of the local spin density (LSD) functional theory.[20] This method has been described in detail elsewhere.[21,22] In our calculations, the exchange and correlation term takes the form deduced by Von Barth and Hedin.[23] s, p, and d orbitals are used for Fe, Ni, and Mn atoms, and s, p, d, and f orbitals are used for La atoms. The atomic sphere radii are chosen using an automatic procedure developed by Krier *et al.*[24] in such a way that space filling is achieved without exceeding two atomic spheres overlap of 16%. Both down folding techniques[25] and the tetrahedron method[26] have been used in the calculation. The calculation is performed for 512 k points in the irreducible parts of the Brillouin zone. The atomic positions of $LaNi_{5-x}Fe_x$ and $LaNi_{5-x}Mn_x$ are scaled according to our experimental results shown in Fig. 2. Convergence is assumed when the root-mean-square error of the self-consistent total energy E_{total} is smaller than 10^{-6} Ry.

The calculations have been performed for $LaNi_{5-x}T_x$ (T = Fe, Mn) with $x=0.5$, 1.0, 1.5, 2.0, and 3.0. For $x=0.5$ and 1.5, supercells with La_2Ni_9T and $La_2Ni_7T_3$ have been used (see Table II). For $LaNi_{5-x}Fe_x$ with $x=2.0$ and 3.0, due to the fact that experimental lattice parameters are not available, we have linearly extrapolated the experimental data and obtained lattice paramters of $a=5.081$ Å, $c=4.049$ Å, and $a=5.202$ Å, $c=4.097$ Å. For $LaNi_{5-x}Mn_x$ with $x=3.0$, the extrapolated lattice paramters are $a=5.312$ Å, $c=4.221$ Å.

In order to study the site preference, the total energy of the unit cell was calculated for Fe and Mn atoms occupying different crystallographic sites, namely, $2c$ or $3g$. The Mn atoms in the $3g$ sites have been assigned as $3g$-1, $3g$-2, and $3g$-3, which are assumed as magnetically inequivelant due to the ferrimagnetic or antiferromagnetic structures of the Mn containing compounds. The total energies were also calculated when the magnetic moments of Mn atoms in the $3g$ sites are antiferromagnetically or ferromagnetically coupled.

From self-consistent charge density calculated, the Fermi contact hyperfine fields H_{FC} of $LaNi_{5-x}Fe_x$ and $LaNi_{5-x}Mn_x$ were calculated according to the prescription given by Akai *et al.* for scalar-relativistic calculations.[27] For the scalar-relativistic wave functions used in the hyperfine field calculation, the effective spin density at the nucleus was computed following Ref. 28 by averaging over a small region near the nucleus with a diameter of $r_T=\mathrm{Ze}^2/\mathrm{mc}^2$ (r_T is Thomson radius, Z is nuclei charge number).

IV. ELECTRONIC STRUCTURES AND HYPERFINE INTERACTIONS

Figure 4 shows the total densities of states (DOS) for $LaNi_{5-x}Fe_x$ ($x=0.0$, 1.0, 2.0, and 3.0). $LaNi_5$ is paramagnetic, and the Fermi level lies near the minimum of the total DOS. After Fe substitution, the total DOS of all the compounds show exchange splitting, and the Fermi level lies

TABLE II. The calculated magnetic moments (μ_B) of atoms in $LaNi_{5-x}Mn_x$ ($x=0.5$, 1.0, 1.5, 2.0, and 3.0).

x	0.5	1.0		1.5		2.0		3.0
	Theor.	Theor.	Expt.	Theor.	Expt.	Theor.	Expt.	Theor.
La($1a$)	−0.06	−0.14	0	−0.03	0	0	0	−0.09
Ni($2c$)	0.11	0.23	0.21	0.11	0.09	0	0.04	0.13
Ni($3g$)	0.12	0.27	0.14	0.24	0.11	0	0.06	
Mn($3g$-1)	2.98	3.14	3.25	3.03	3.0	3.11	2.45	3.14
Mn($3g$-2)				−3.33	−3.0			−3.31
Mn($3g$-3)				3.03	3.0	−3.11	−2.45	3.14

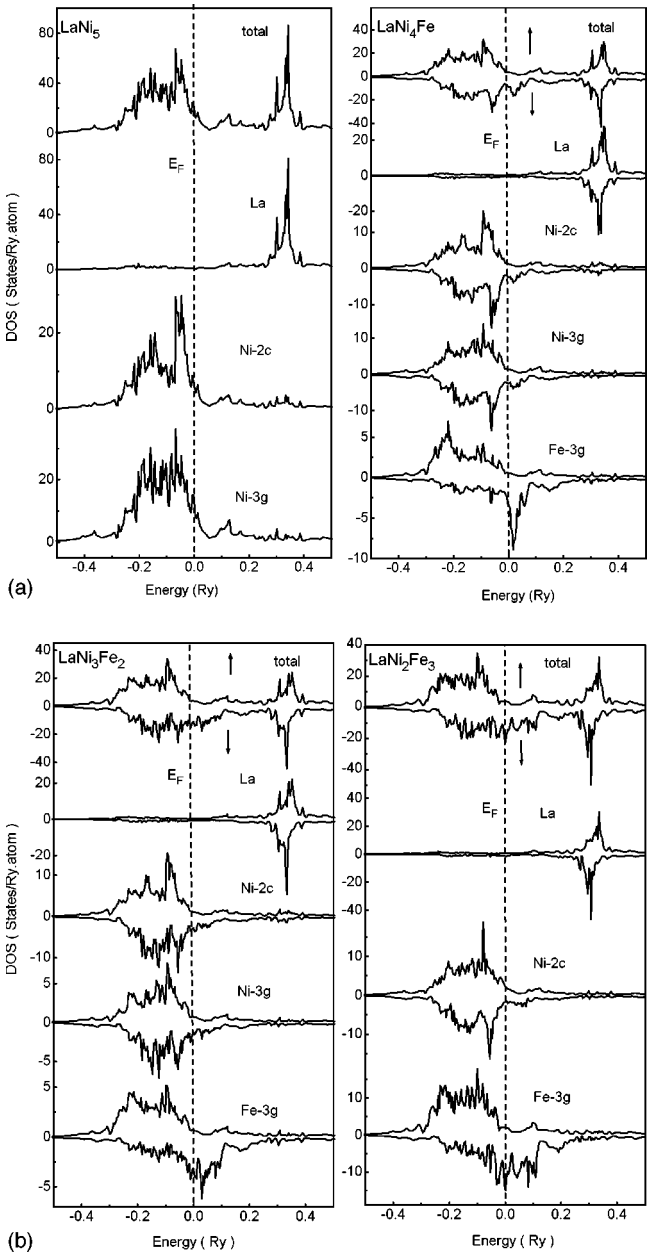

FIG. 4. Total densities of states of $LaNi_{5-x}Fe_x$ ($x=0.0$, 1.0, 2.0, and 3.0).

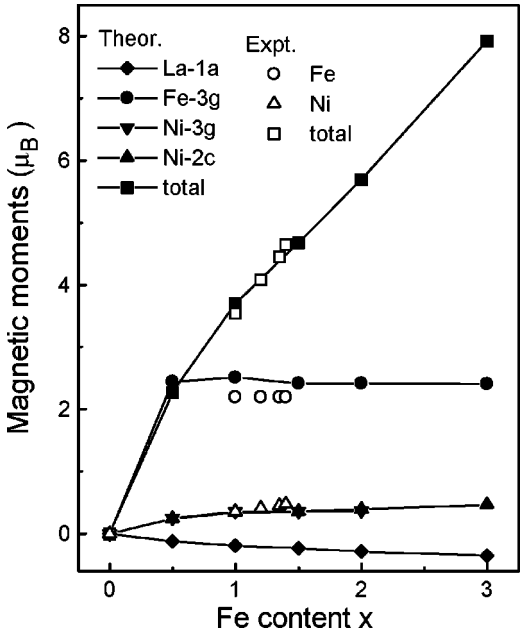

FIG. 5. The calculated magnetic moments of different atoms in $LaNi_{5-x}Fe_x$ and total magnetic moments in a unit cell. The hollow symbol represents the experimental values which were measured in a magnetic field of 6 T by using SQUID.

above the top of spin up DOS. As expected, the DOS are dominated by the Fe and Ni d bands near the Fermi level. The DOS shape of the Ni atoms becomes broader after Fe substitution as compared with that in $LaNi_5$, and shows a dependence on the Fe contents due to the interaction between the Fe and Ni atoms. The Fermi level lies nearly above the top of both the spin up and spin down DOS of the Ni atoms, and a very small exchange splitting was observed. The spin down DOS of the Fe consists of one peak for $x=0.5$ and 1.0 compounds, but a continuous region is formed as the Fe content increases. This is a consequence of the interactions between Fe-Fe, Fe-Ni, and Fe-La broadening the Fe-3d bands. The calculated magnetic moments of the different atoms and the total magnetic moments for $LaNi_{5-x}Fe_x$ are shown in Fig. 5. As a comparison, we have included some available experimental data in this figure. The calculated results are in good agreement with the experimental results. Fe atoms possess magnetic moments as large as $2.5\mu_B$ due to a very large exchange splitting and strong ferromagnetic characteristics. Since $LaNi_5$ is paramagnetic, then due to the dilution effect, the Fe d bands tend to be narrower and more localized when the Fe concentration is low. This can explain why the magnetic moments of the Fe atoms are higher than those of α-Fe. Ni atoms have magnetic moments in the range of $0.2–0.5\mu_B$. The magnetic moments of the Ni atoms increase with Fe content, which is in agreement with the neutron refinement data. The La atoms have a negative moment which is induced by the Fe atoms.

The calculated hyperfine fields of the different atoms are shown in Fig. 6. As a comparison, some available experimental hyperfine fields are shown also in Fig. 6. Again, the calculated results agree well with experimental data.[13] Further, the hyperfine field can provide us with more details of electron interactions in the compounds. We decompose H_{FC} into two parts $H_{\mathrm{FC}}^{\mathrm{core}}$, which is the contribution of the core electrons and comes from the polarization of the core due to the polarized d electrons and $H_{\mathrm{FC}}^{\mathrm{val}}$, which comes from the polarization of the valence electrons. The $H_{\mathrm{FC}}^{\mathrm{core}}$ and $H_{\mathrm{FC}}^{\mathrm{val}}$ contributions of H_{FC} are also shown in Fig. 6. The $H_{\mathrm{FC}}^{\mathrm{val}}$ values of Fe atoms are higher than the normal values of the 3d metals (-5 T), and have positive signs.

The magnetic moment (μ_{loc}) dependence of the H_{FC}, $H_{\mathrm{FC}}^{\mathrm{core}}$, and $H_{\mathrm{FC}}^{\mathrm{val}}$ at Fe sites is shown in Fig. 7. Obviously, a linear relationship between the $H_{\mathrm{FC}}^{\mathrm{core}}$ and local magnetic moments is observed, and the proportionality coefficient is estimated to be about $-15T/\mu_B$, whereas the valence contribution and total hyperfine field are not proportional to the

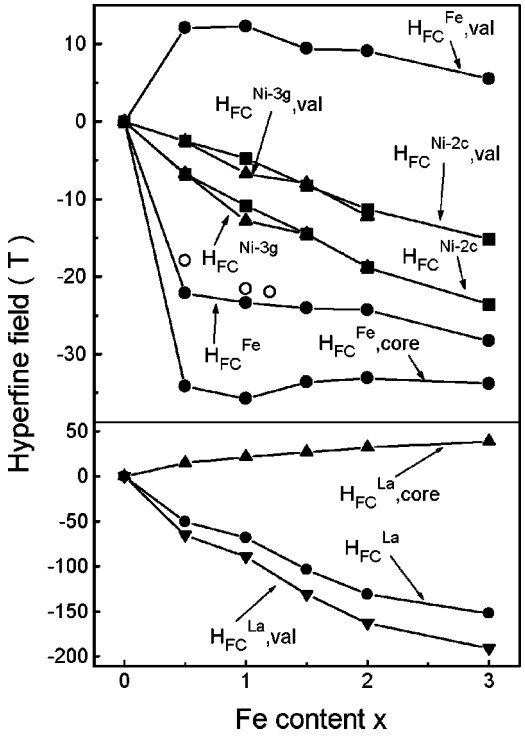

FIG. 6. The calculated hyperfine fields of different atoms in $LaNi_{5-x}Fe_x$. The hollow circles represent the experimental hyperfine fields which are taken from Ref. 13.

magnetic moments. This is the reason why the magnetic moments obtained from Mösssbauer measurements in Ref. 13 are much lower than the magnetic measurements data, though the transfer factor (14.5 T/μ_B) is almost the same in our result (15 T/μ_B). Hence, it can be seen that $H_{\rm FC}$ at the Fe sites is affected by two factors, $\mu_{\rm loc}$ and the polarization of the valence electrons. Therefore estimations of the magnetic moments from the hyperfine field are not totally correct

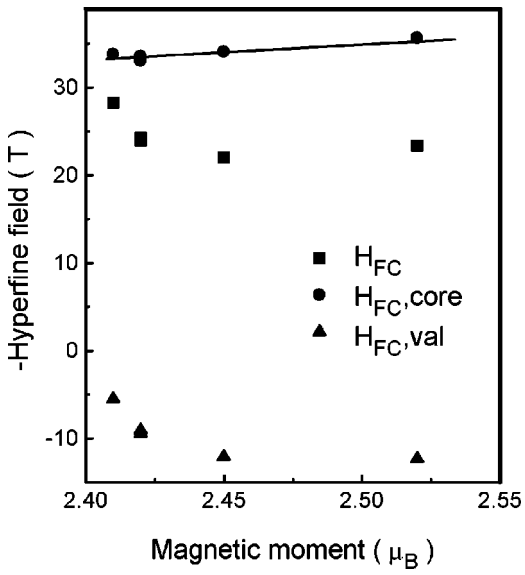

FIG. 7. The dependence of $H_{\rm FC}^{\rm core}$ and $H_{\rm FC}^{\rm val}$ at Fe sites on Fe magnetic moments ($\mu_{\rm Fe}$) in $LaNi_{5-x}Fe_x$.

if one uses a proportionality factor, especially when compounds have a large valence hyperfine field.

$H_{\rm FC}^{\rm val}$ consists of two terms, one is the local valence hyperfine field $H_{\rm FC}^{l,{\rm val}}$ which comes from the *s*-*d* exchange interaction within the atoms and is proportional to the local magnetic moments μ_s of the *s* electrons (normally it is positive); another is the transferred hyperfine field $H_{\rm FC}^{t,{\rm val}}$ which comes from the *s*-*d* hybridization between the *s* orbitals of the atoms and the spin-polarized *d* orbitals of the neighboring atoms. Normally, this term is negative. Thus $H_{\rm FC}^{\rm val}$ may reveal *s*-*d* hybridization among the metal atoms. As evidenced in Fig. 6, very large positive values of $H_{\rm FC}^{\rm val}$ for Fe atoms were obtained, suggesting a strong *s*-*d* hybridization occurring within the Fe atoms that decreases with increasing Fe content. This effect causes Fe 3*d* electrons to be more localized and have higher magnetic moments, especially when Ni is substituted by a small amount of iron ($x \leqslant 1.0$). For the Ni and La atoms, the valence hyperfine fields are negative and dominate $H_{\rm FC}$, meaning that the Ni and La *s* electrons are strongly polarized by neighboring Fe *d* moments via the Ruderman-Kittel-Kasuya-Yosida (RKKY-) like mechanism. This interaction may lead to an oscillating spin density of the *s* electrons and could be the reason some magnetic clusters are coupled by an RKKY-like interaction resulting in the spin freezing observed in $LaNi_{5-x}Fe_x$.[14,15] Here, because $LaNi_5$ is paramagnetic, the RKKY-like interaction will be very important only when a small mount of Ni is substituted by Fe. For higher Fe concentrations, this system undergoes a transition to ferromagnetic ordering.[17]

In order to check the site preference of Mn in $LaNi_{5-x}Mn_x$ compounds, we have performed the total energy calculation when the Mn atoms occupy different sites. The calculated total energy for Mn occupying 2*c* sites is 9 mRy higher than that for Mn occupying 3*g* sites, which means it is more stable for Mn to occupy the 3*g* sites. The calculated total energies of Fe-substituted compounds also indicate that the Fe atoms prefer the 3*g* sites. The total energy is 8 mRy higher for one Fe atom occupying the 3*g* sites than that in 2*c* sites. Antiferromagnetic or ferrimagnetic exchange between Mn in the 3*g* sites is presented when 2 or 3 Mn atoms are located in these sites. This agrees with the neutron refinement, where a ferrimagnetic (antiferromagnetic) model gives the best fit for $x=2.0$, while a ferromagnetic model gives the best fit for $x=1.0$.

The DOS of $LaNi_{5-x}Mn_x$ ($x=1.0$, 2.0 and 3.0) are shown in Fig. 8. The most interesting thing is the magnetic interaction feature between Mn atoms in these compounds. The DOS shape of Mn is dependent on the number of the Mn atoms in a unit cell. All Mn atoms have a large exchange splitting indicating strong ferromagnetic character. The Fermi level is located above the top of the spin up DOS, and is just below the main peak of the spin down DOS, which results in a magnetic moments of $3\mu_B$ per Mn. The Fermi level is almost above the top of both the spin up and spin down DOS of all the Ni atoms, so that a very small magnetic moment is produced. When $x=2$, the antiferromagnetic coupling between two Mn atoms on the 3*g* sites causes a zero magnetic moment on both the Ni and La atoms. When *x*

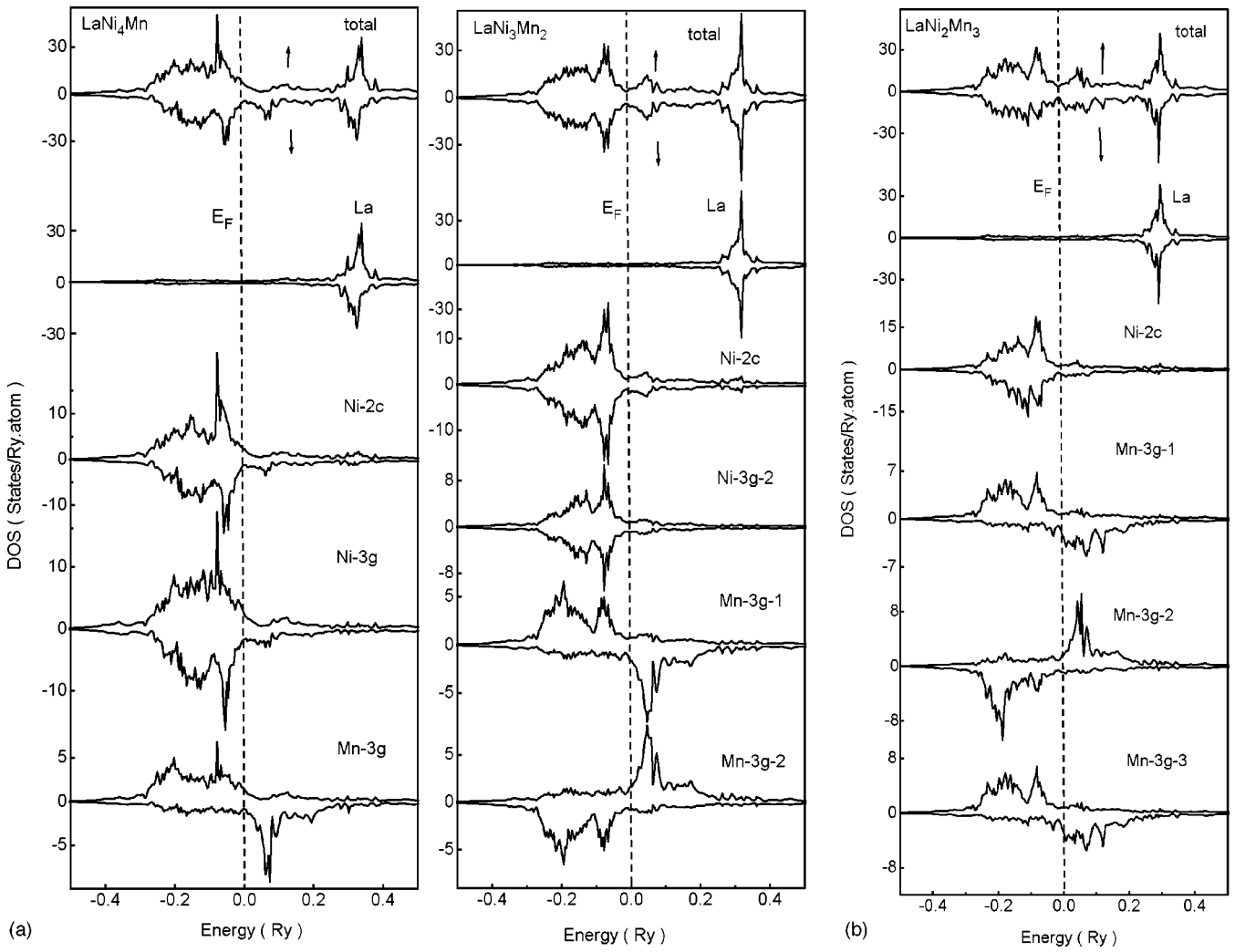

FIG. 8. Total densities of states of $LaNi_{5-x}Mn_x$ ($x=1.0$, 2.0, and 3.0).

$=3$, a ferrimagnetic structure is formed as shown in the DOS. The calculated magnetic moments of these compounds are listed in Table III. For comparison, we have included some experimental data. Again, the theoretical results agree with the neutron refinement data. Here we should point out that for the Mn-substituted samples, the magnetic structures of the compounds depend on the number of Mn atoms in these compounds. For $LaNi_{5-x}Mn_x$, $x=2$ results in an antiferromagnetic structure, and $x=3$ leads to a ferrimagnetic structure, whereas $x=1.0$ is ferromagnetic. The calculated hyperfine fields of Mn are listed in Table III. Similar to $LaNi_{5-x}Fe_x$, a large valence contribution to the hyperfine field was found for Mn atoms due to the strong *s-d* localized hybridization within Mn atoms. La and Ni atoms also show large valence transferred hyperfine fields, as mentioned above, which indicates that the Ni-Mn and La-Mn interactions have a RKKY-like mechanism. This could be the reason for spin freezing in $La(Ni,Mn)_5$ compounds.[12]

TABLE III. The calculated hyperfine fields (T) of atoms in $LaNi_{5-x}Mn_x$ ($x=0.5$, 1.0, 1.5, 2.0, and 3.0).

x	0.5		1.0		1.5		2.0		3.0	
	H_{FC}	H_{FC}^{val}	H_{FC}	H_{FC}^{val}	H_{FC}	H_{FC}^{val}	H_{FC}	H_{FC}^{val}	H_{FC}	H_{FC}^{val}
La(1*a*)	−52.0	−59.6	−113.0	−129.7	−43.2	−47.7	0	0	−76.5	−65.8
Ni(2*c*)	−0.6	−0.4	−11.7	−7.5	−5.2	−4.5	0	0	−11.7	−9.4
Ni(3*g*)	−3.3	−2.1	−13.6	−9.9	−4.3	−3.4	0	0		
Mn(3*g*-1)	−20.0	18.4	−23.1	17.9	−23.8	15.5	−13.8	26.7	−17.4	23.3
Mn(3*g*-2)					20.2	−22.9	13.8	−26.7	4.9	−37.6
Mn(3*g*-3)					−23.8	15.5			−17.4	23.3

V. CONCLUSIONS

A systematic study of the magnetic moments and hyperfine interactions of the $LaNi_{5-x}Fe_x$ and $LaNi_{5-x}Mn_x$ compounds was performed using the LSD approximation and the TB-LMTO-ASA method. The calculated results were compared with neutron diffraction data and found to be in good agreement. Fe atoms exhibit more localized magnetic moments in $LaNi_{5-x}Fe_x$ when the Fe content x is lower than 1.0. The calculated magnetic moments of Fe approach values as large as $2.5\mu_B$ due to the dilution effect. The strong s-d hybridization between the Ni and La atoms and the neighbor Fe(Mn) in the Fe(Mn)-substituted samples results in a large transferred valence contribution to the total hyperfine field. This s-d hybridization confirms that some magnetic clusters are coupled by an RKKY-like interaction in the $LaNi_{5-x}Fe(Mn)_x$ compounds with low Fe(Mn) content at low temperatures. Both Fe and Mn atoms prefer to locate at the $3g$ sites. The Mn-substituted samples exhibit both antiferromagnetic and ferrimagnetic structures depending upon the number of Mn atoms in one unit cell. A magnetic moment of $3\mu_B$ per Mn is calculated for the $LaNi_{5-x}Mn_x$ compounds.

ACKNOWLEDGMENTS

The financial support of the National Science Foundation for Grants No. DMR-9614596 and the Defense Advanced Research Projects Agency for Grant No. DAAG 55-98-1-0267 is acknowledged. One of the authors (J.B.Y.) thanks Dr. O. Jepsen of the Max-Planck-Institut, Stuttgart, Germany for his help and providing the TB-LMTO code.

[1] K. H. J. Buschow, *Ferromagnetic Materials* edited by E. P. Wohlfarth (North Holland, Amsterdam, 1988) Vol. 1, p. 297.
[2] H. S. Li and J. M. D. Coey, *Handbook of Magnetic Materials*, edited by K. H. Buschow (North-Holland, Amsterdam, 1991), p. 1, and references therein.
[3] J.P. Liu, F.R. de Boer, P.F. de Chatel, R. Coehoorn, and K.J. Buschow, J. Magn. Magn. Mater. **132**, 159 (1994).
[4] J. J. M. Franse and R. J. Radwanski, *Handbook of Magnetic Materials*, edited by K. H. Buschow (Elsevier, Amsterdam, 1993), p. 307.
[5] *Hydrogen in Metals*, edited by G. Alefeld and J. Völk (Springer, Berlin, 1978), Vols. 1,2.
[6] D. Shaltiel, J.H. Wernick, H.J. Williams, and M. Peter, Phys. Rev. **135**, A1356 (1964).
[7] A.M. Van Diepen, K.H.J. Bushcow, and J.S. Van Wieringen, J. Appl. Phys. **43**, 645 (1972).
[8] E. Wallace, *Rare Earth Intermetallics* (Academic, New York, 1973), pp. 181–188.
[9] A. Percheron-Guegan, C. Lartigue, J.C. Archard, P. Germi, and T. Tasset, J. Less-Common Met. **74**, 1 (1980); **75**, 23 (1980).
[10] C. Lartige, A. Percheron-Guegan, J. C. Archard, and F. Tassett, in *Rare Earth in Modern Science and Technology*, edited by G. J. McCarthy, J. J. Rhyne, and H. B. Silber (Plenum, New York, 1980), Vol. 2, p 585.
[11] S.J. Campbell, R.K. Day, J.B. Dunlop, and A.M. Stewart, J. Magn. Magn. Mater. **31-34**, 167 (1983).
[12] F.T. Parker and H. Oesterreicher, J. Magn. Magn. Mater. **36**, 195 (1983).
[13] J. Lamloumi, A. Percheron-Guegan, J.A. Achard, G. Jehanno, and D. Givord, J. Phys. (France) **45**, 1643 (1984).
[14] M. Escorne, J. Lamloumi, A. Percheron-Guegan, J.A. Achard, A. Mauger, and G. Jehanno, J. Appl. Phys. **45**, 4121 (1988); J. Magn. Magn. Mater. **65**, 63 (1987).
[15] M. Escorne, A. Mauger, J. Lamloumi, and A. Percheron-Guegan, Solid State Commun. **89**, 761 (1994).
[16] M. Gerlach, N. Mommer, M. Hirscher, and H. Kronmüller, J. Alloys Compd. **267**, 47 (1998).
[17] C.Y. Tai, C. Tan, G.K. Marasinghe, O.A. Pringle, W.J. James, M. Chen, W.B. Yelon, J. Gebhardt, and N. Ali, IEEE Trans. Magn. **35**, 3346 (1999).
[18] C.Y. Tai, G.K. Marasinghe, O.A. Pringle, W.J. James, M. Chen, W.B. Yelon, I. Dubenko, N. Ali, and Ph. I'heritier, J. Appl. Phys. **87**, 6731 (2000).
[19] J. Rodriguez-Carvajal, PROGRAM: FULLPROF, version 3.0.0, 1995.
[20] O. K. Anderson, O. Jepsen, and M. Snob, in *Linearized Band Structure Methods in Electronic Band Structure and Its Applications, Lecture Notes in Physics* (Springer, Berlin, 1987).
[21] O.K. Anderson and O. Jepsen, Phys. Rev. Lett. **53**, 2571 (1984).
[22] O.K. Anderson, Z. Pawlowska, and O. Jepsen, Phys. Rev. B **34**, 5253 (1986).
[23] U. von Barth and L. Hedin, J. Phys. C **5**, 1629 (1972).
[24] G. Krier, O. K. Anderson, and O. Jepsen (unpublished).
[25] W.R.L. Lambrecht and O.K. Anderson, Phys. Rev. B **34**, 2439 (1986).
[26] O. Jepsen and O.K. Anderson, Solid State Commun. **9**, 1763 (1971); Phys. Rev. B **29**, 5965 (1984); P. Blöchl, O. Jepsen, and O.K. Anderson, *ibid.* **49**, 16 223 (1994).
[27] H. Akai, M. Akai, S. Blügel, B. Drittler, E. Ebert, K. Terakura, R. Zeller, and P.H. Dederichs, Prog. Theor. Phys. Suppl. **101**, 11 (1990).
[28] S. Blügel, H. Akai, R. Zeller, and P.H. Dederichs, Phys. Rev. B **35**, 3271 (1987).